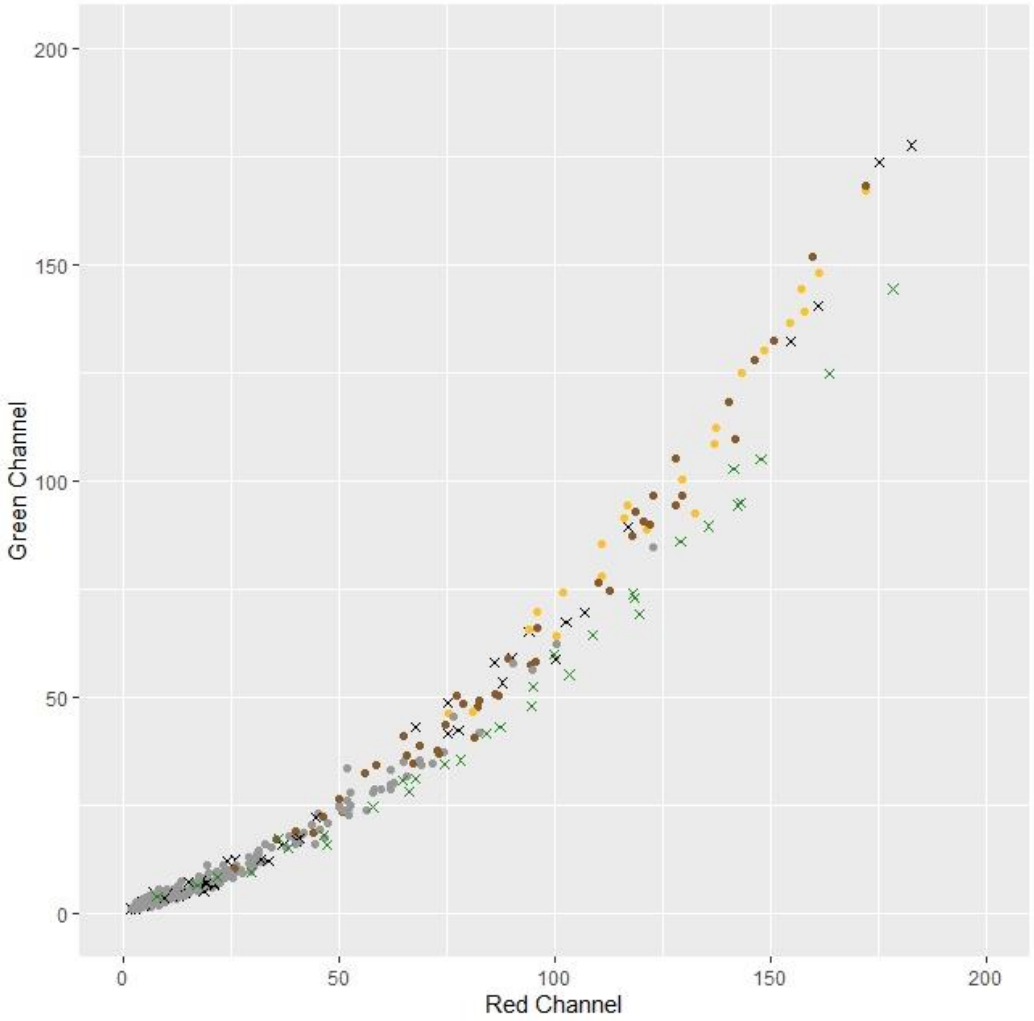

Figure S1- Hair reflectance of *Ursus americanus* and *U. arctos*. Related to Figure 1A, 2A, and 4.
Hair reflectance scores for the red (x-axis) and green (y-axis) channels for *Ursus americanus* and *U. arctos*. Sample data for *U. americanus* is colored by $TYRP1^{R153C}$ genotype, including: homozygous ancestral (GG; grey), heterozygous (GA; brown), homozygous derived (AA; gold), and no genotype data (black "X"); whereas, all *U. arctos* samples are shown as green "X."

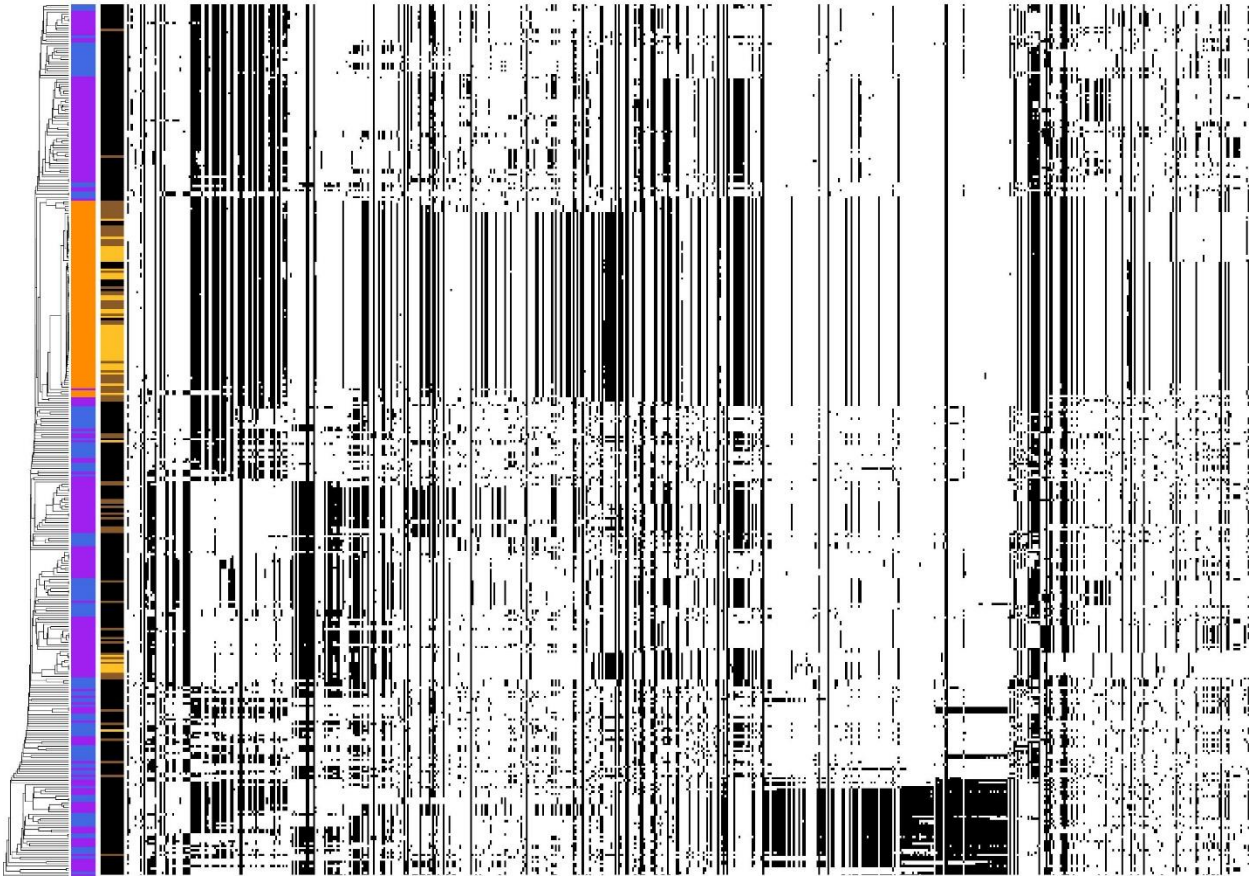

Figure S2- Haplotypes of American black bears spanning the causative locus for brown coloration. Related to Figure 2B.

Ursus americanus haplotypes from phased high and low coverage WGS (see Table S1) on scaffold 24 encompassing the 97kb haplotype identified in the Nevada population containing *TYRP1*. Alternate alleles shown as black lines for each sample (represented as a row). Relationships among haplotypes represented as a gene tree on far left, geographic location of samples noted by leftmost colored bar (western lineage: orange; Southeast Alaska: purple; eastern lineage: blue), and qPCR genotype of R153C represented by rightmost colored bar (homozygous ancestral: black; heterozygous: brown; homozygous derived: gold).

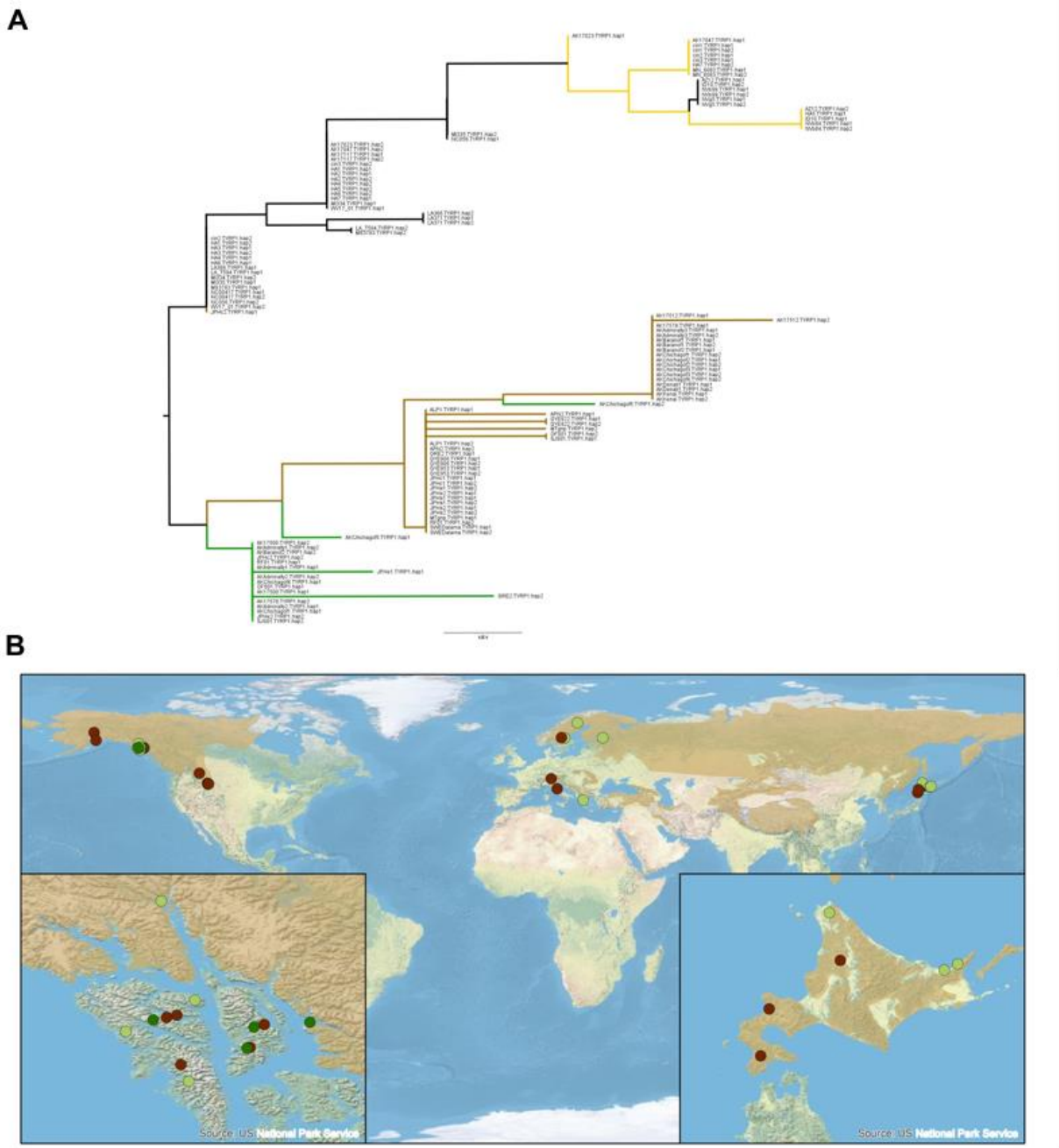

Figure S3- Phylogenetic and geographic distribution of *U. arctos TYRP1* haplotypes. Related to Figure 3.

(A) Unrooted neighbor joining haplotype tree of *Ursus americanus* and *U. arctos TYRP1* haplotypes (including exons and introns). Haplotypes carrying causative variants within *TYRP1* are denoted by color with *U. americanus* (American black bear) in black (R153 ancestral allele) or gold (C153 derived allele), and *U. arctos* in brown (R114 ancestral allele) or green (C114 derived allele). (B) Map of the global distribution of R114C in *U. arctos* individuals sequenced to high coverage (see Key Resources Table), where brown circles indicate homozygous ancestral, light green are heterozygous individuals, and dark green are homozygous derived. The derived allele frequency from 32 global samples is 0.297. Left inset map highlights Southeast Alaska, USA; right inset map highlights Hokkaido, Japan. Brown shading indicates the current species distribution.

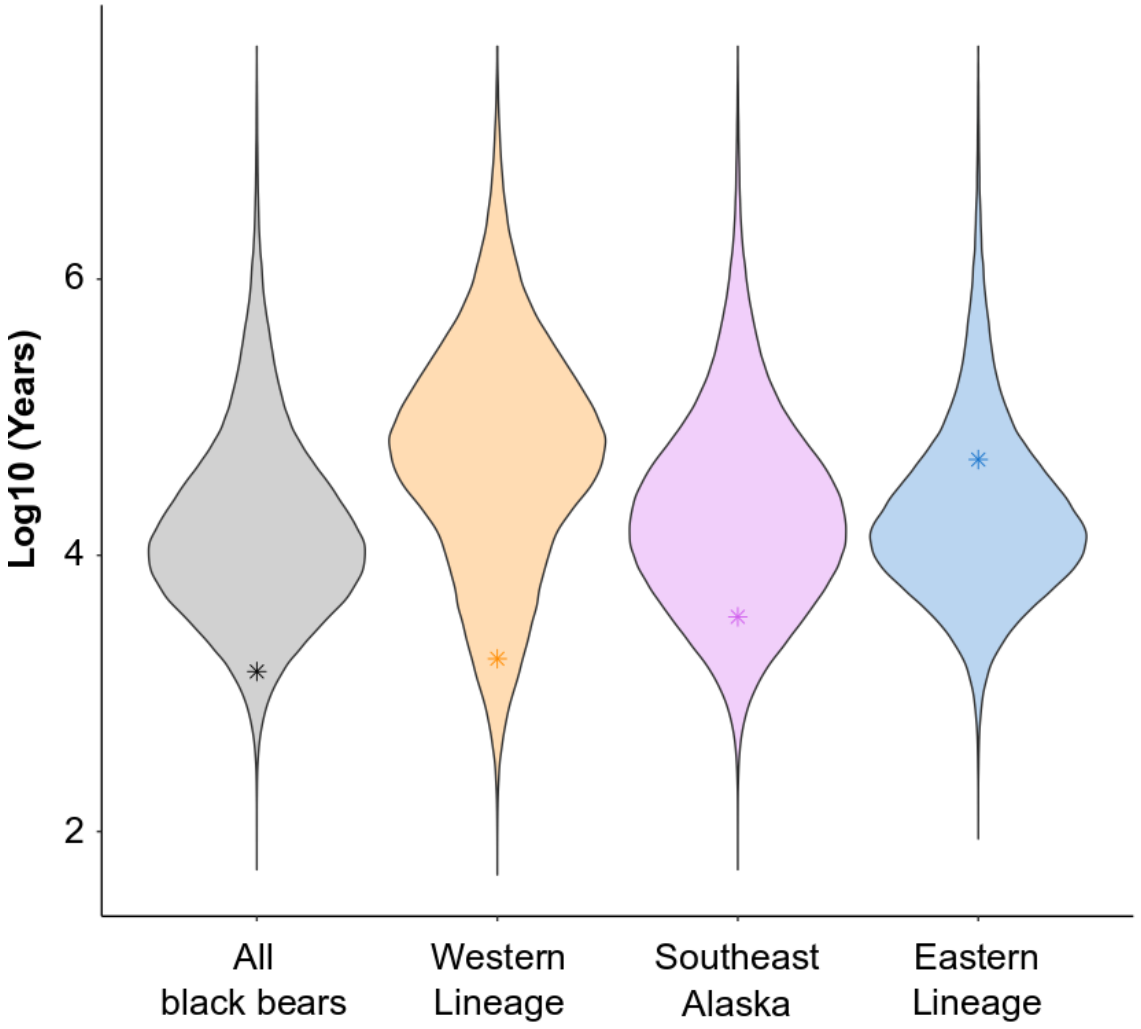

Figure S4- Distribution of coalescent estimates on the scaffold containing *TYRP1*. Related to Figure 5. Coalescence time estimates from all variants on *Ursus americanus* scaffold 24 for all samples (grey; n = 185), western lineage (overrepresented by the Nevada population; orange; n = 44), Southeast Alaska population (purple; n = 84), and eastern lineage (blue; n = 57). The star (*) within each violin plot represents the estimate of the *TYRP1* R153C causative variant.

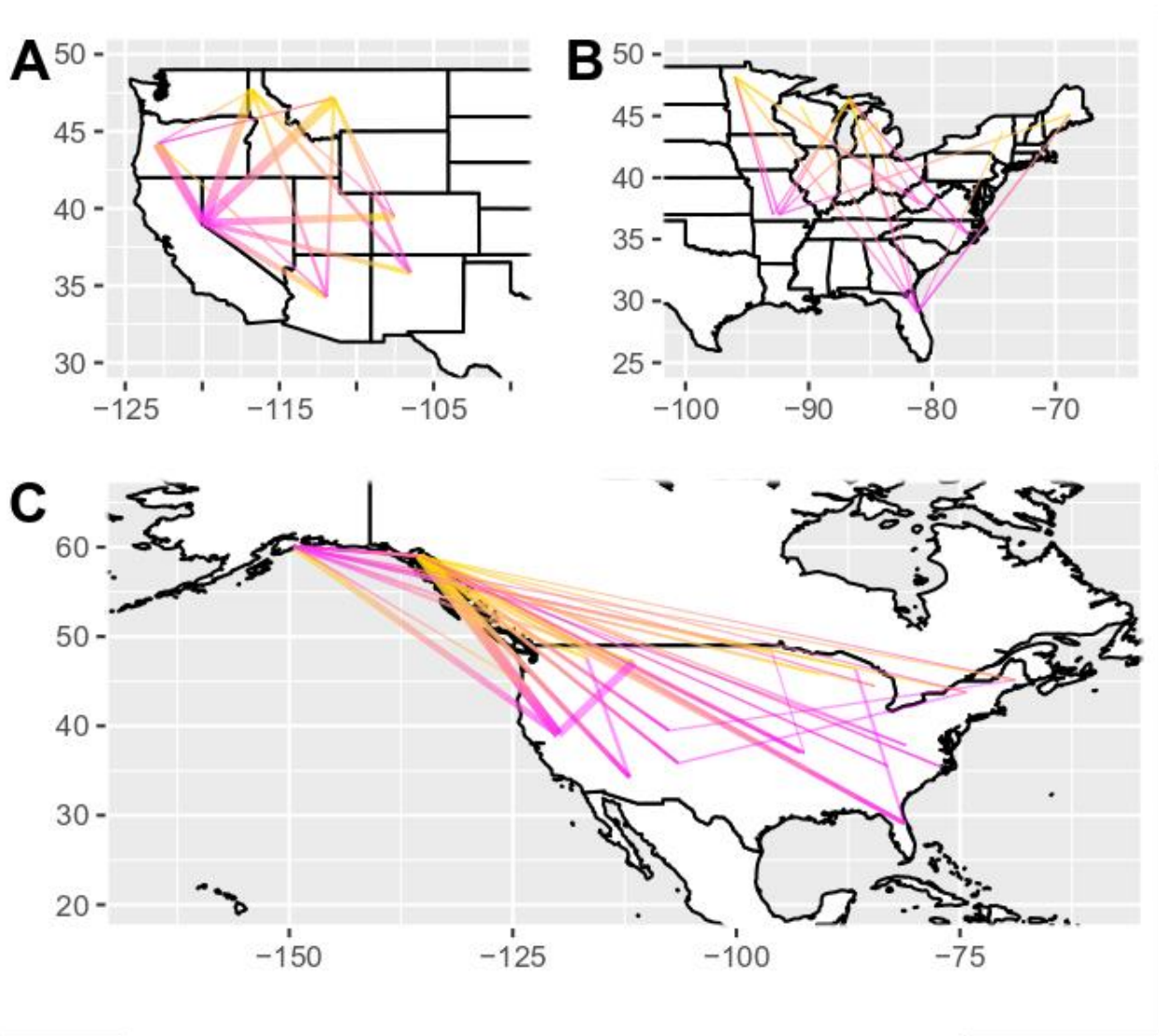

Figure S5- Directional range expansion of American black bears. Related to Figure 5C.
Estimates of regional *Ursus americanus* range expansions based on pairwise ψ statistics (A) within the western lineage populations, (B) within the eastern lineage populations, and (C) among the western and eastern lineages and Alaskan (both Southeast and Kenai) populations. Lines show directionality from inferred source (magenta) to sink (gold) populations, where thickness was scaled to the *Z*-score when the absolute value was greater than five.

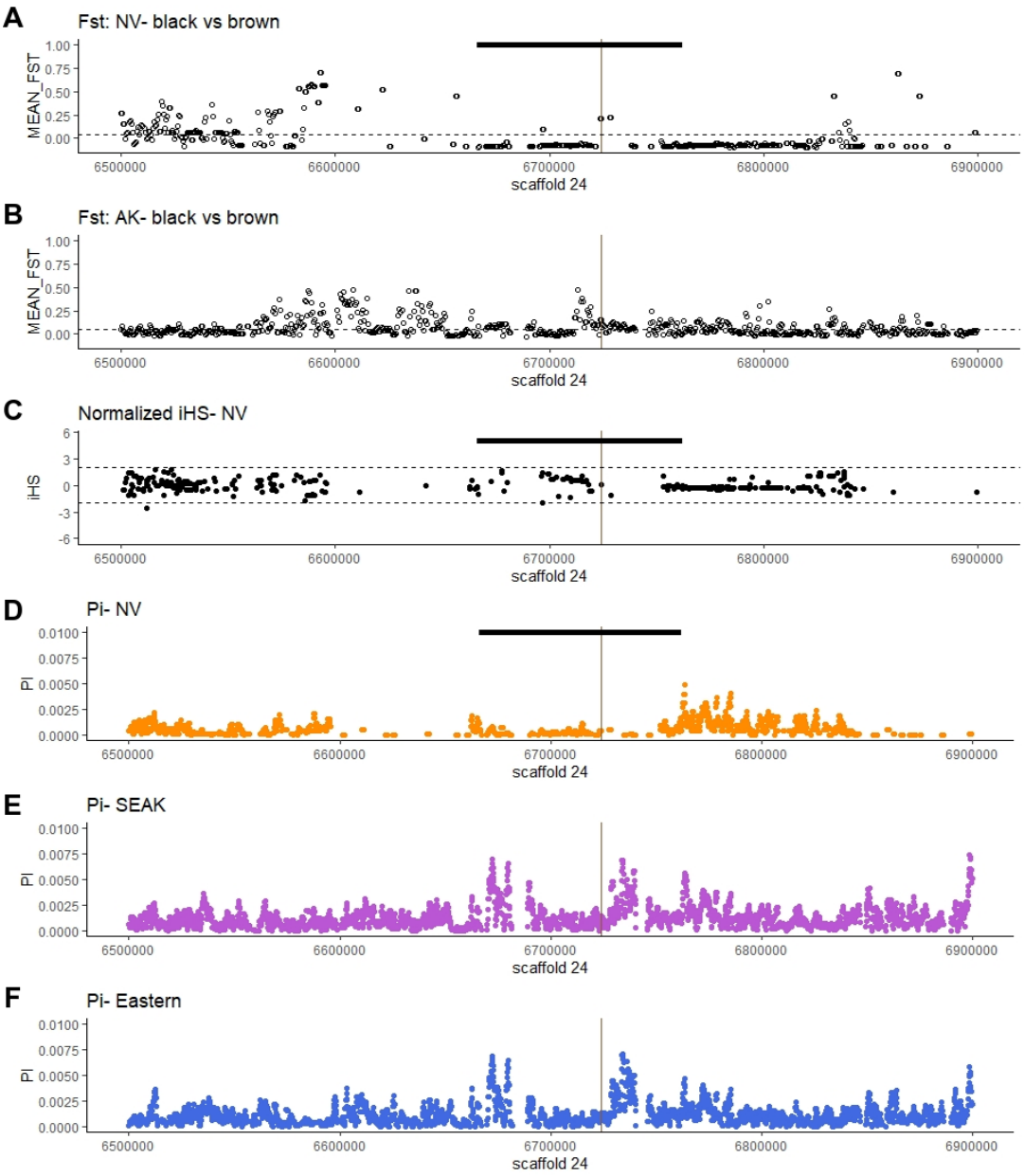

Figure S6- Population genetic statistics surrounding *TYRP1*. Related to the Star Methods.
(A, B) Genetic differentiation (F_{ST}), (C) selection (integrated haplotype score, iHS), and (D-F) genetic diversity across scaffold 24 of the *Ursus americanus* genome. (A, B) Pairwise F_{ST} estimates in sliding windows (1,000bp window; 100bp slide) between black and brown coated animals within either the Nevada (NV; A) or Southeast Alaskan (SEAK; B) populations, where average F_{ST} for the scaffold is indicated by the dashed line. (C) iHS was calculated in sliding windows (10k window, 2.5k slide) across scaffold 24 and normalized by allele frequency using selscan. The dashed lines represent iHS scores of |2| which is considered significant. (D-F) Nucleotide diversity within three different populations (D: NV in the western lineage; E- SEAK; F- Appalachian Mountains in the eastern lineage) of *U. americanus* along scaffold 24. Diversity is low across the haplotype regardless of coat color phenotype. In each panel, the vertical line represents the position of the R153C allele. The thick black bar in panels of the Nevada population show the length of the 97kb haplotype identified.

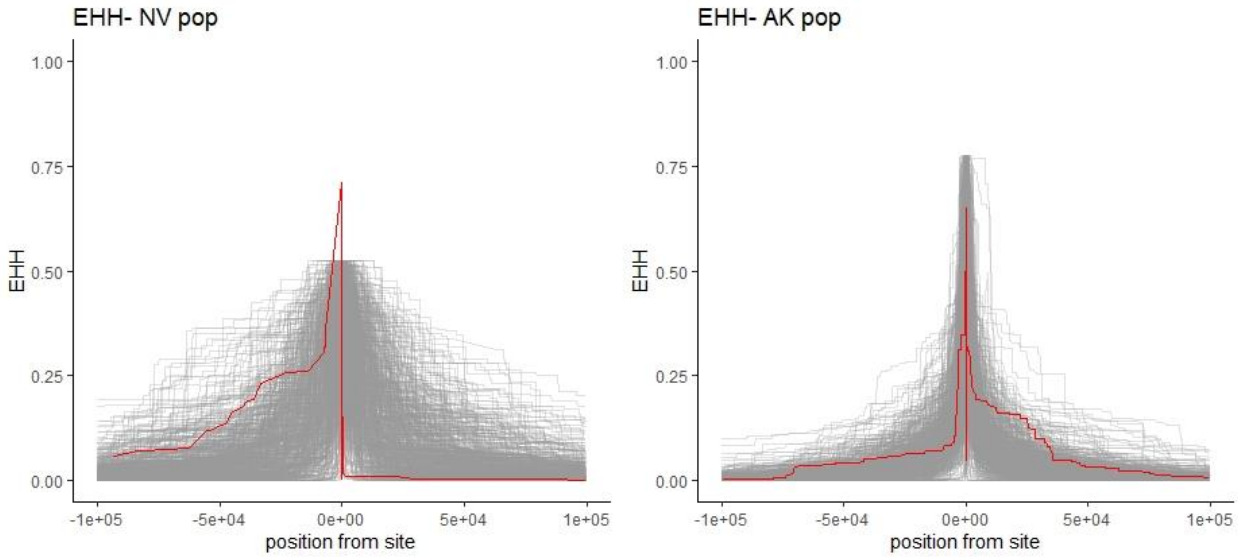

Figure S7- Population specific extended haplotype homozygosity analysis. Related to the Star Methods.

Extended haplotype homozygosity (EHH) of the causative *TYRP1*^{R153C} allele (red line) in both the Nevada (left) and SEAK (right) populations compared to 540 allele frequency matched sites from throughout the genome of *Ursus americanus*.

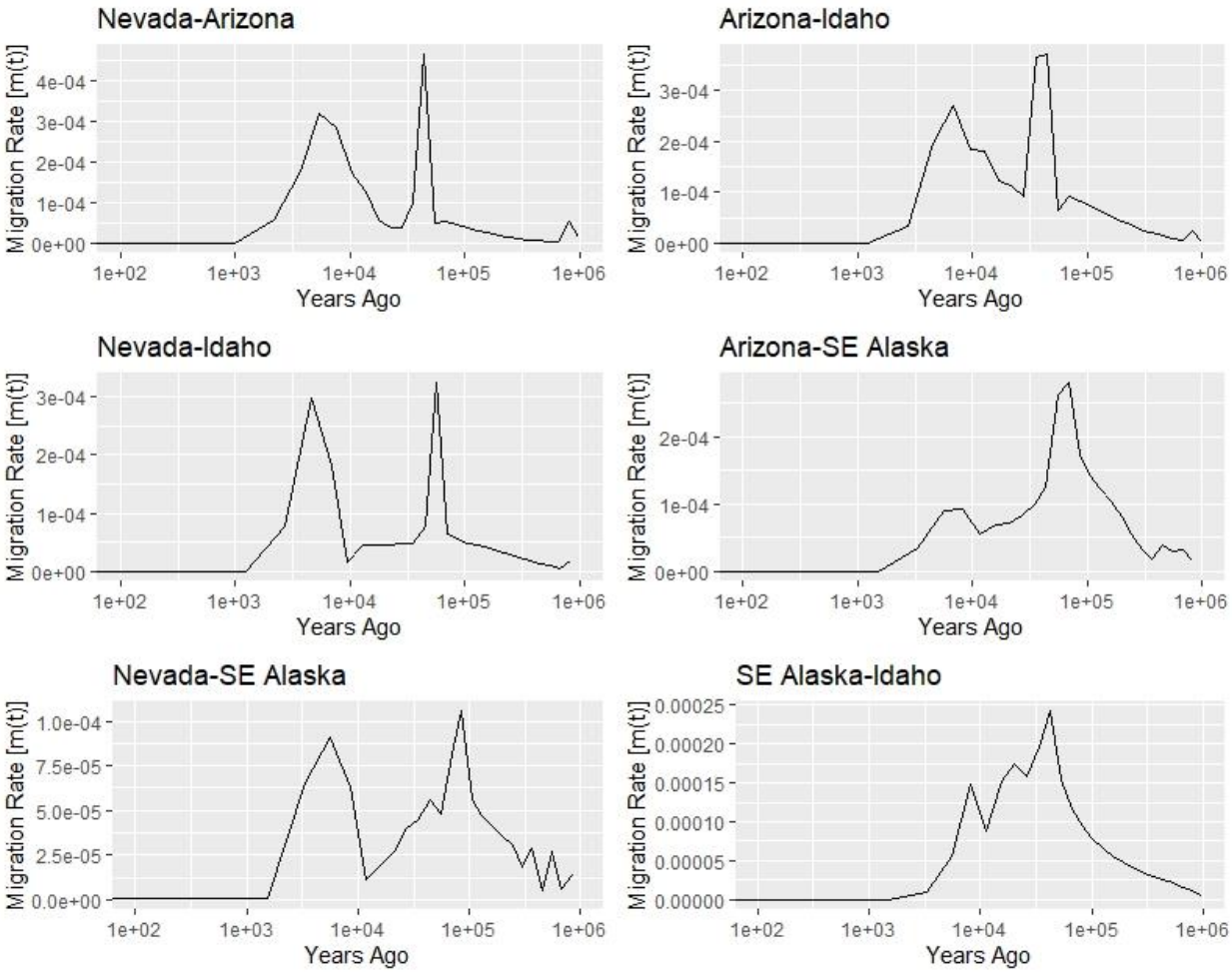

Figure S8- Rates of gene flow through time in four American black bear populations. Related to Figure 6.

Estimated historic gene flow among four populations (Nevada, Arizona, Idaho, and Southeast Alaska) based on MSMC-IM estimates from a single WGS genome per population. The peak bidirectional migration between each population was used as the rate within the SLiM3 forward simulation models.

SUPPLEMENTAL TABLES

Table S1- Data for reflectance values and chemical analysis. Relates to Figure 1. Individual *Ursus americanus* and *U. arctos* used for high (hcWGS) and low (lcWGS) coverage whole genome sequencing with NCBI SRA accessions. For animals where hair color reflectance was measured, measured values are listed for the red, green, and blue channels. Animals where hair was not available are listed as "U" for reflectance values. Eumelanin and pheomelanin concentrations are reported as the concentrations of PTCA (pyrrole-2,3,5-tricarboxylic acid) and TTCA (thiazole-2,4,5-tricarboxylic acid), respectively. When known, the sampling location is provided as the longitude and latitude. Sex of the animal listed as male (M), female (F), or unknown (U) based on field biologist calls.

Table S2- Description of GWAS peaks. Relates to Figure 2A. All GWAS hits for brown color in *Ursus americanus* with $P < 10^{-8}$ and annotations of genes under each peak as determined from synteny with human genome on UCSC Genome Browser.

Table S3- Missense and nonsense variants among three species of bears within 13 pigmentation genes. Relates to the Star Methods. Missense and nonsense amino acid substitutions identified (1) within *Ursus americanus*, (2) between *U. americanus* and *U. arctos*, or (3) between *U. arctos* and *U. maritimus* haplotypes for 13 candidate genes. For each variant the Provean, PolyPhen2, and SIFT scores and associated predictions are listed. Values associated with predicted deleteriousness bolded.

Table S4- Bayes Factors for spatial selection analyses. Relates to the Star Methods. Bayes Factors from BayEnv2 testing 15 variables as the potential selective force for the frequency of *TYRP1* R153C among populations across the range of American black bears.

Any use of trade, firm, or product names is for descriptive purposes only and does not imply endorsement by the U.S. Government.

LITERATURE CITED

1. Liu, S., Lorenzen, Eline D., Fumagalli, M., Li, B., Harris, K., Xiong, Z., Zhou, L., Korneliussen, Thorfinn S., Somel, M., Babbitt, C., et al. (2014). Population genomics reveal recent speciation and rapid evolutionary adaptation in polar bears. Cell *157*, 785-794.
2. Benazzo, A., Trucchi, E., Cahill, J.A., Maisano Delser, P., Mona, S., Fumagalli, M., Bunnefeld, L., Cornetti, L., Ghirotto, S., Girardi, M., et al. (2017). Survival and divergence in a small group: The extraordinary genomic history of the endangered Apennine brown bear stragglers. Proceedings of the National Academy of Sciences *114*, E9589-E9597.
3. Cahill, J.A., Green, R.E., Fulton, T.L., Stiller, M., Jay, F., Ovsyanikov, N., Salamzade, R., St. John, J., Stirling, I., Slatkin, M., et al. (2013). Genomic evidence for island population conversion resolves conflicting theories of polar bear evolution. PLoS Genetics *9*, e1003345.
4. Miller, W., Schuster, S.C., Welch, A.J., Ratan, A., Bedoya-Reina, O.C., Zhao, F., Kim, H.L., Burhans, R.C., Drautz, D.I., Wittekindt, N.E., et al. (2012). Polar and brown bear genomes reveal ancient admixture and demographic footprints of past climate change. Proceedings of the National Academy of Sciences *109*, E2382–E2390.
5. Endo, Y., Osada, N., Mano, T., and Masuda, R. (2021). Demographic History of the Brown Bear (Ursus arctos) on Hokkaido Island, Japan, Based on Whole-Genomic Sequence Analysis. Genome Biology and Evolution *13*.
6. Ng, P.C., and Henikoff, S. (2003). SIFT: Predicting amino acid changes that affect protein function. Nucleic Acids Res *31*, 3812-3814.
7. Choi, Y., Sims, G.E., Murphy, S., Miller, J.R., and Chan, A.P. (2012). Predicting the Functional Effect of Amino Acid Substitutions and Indels. PLOS ONE *7*, e46688.
8. Adzhubei, I.A., Schmidt, S., Peshkin, L., Ramensky, V.E., Gerasimova, A., Bork, P., Kondrashov, A.S., and Sunyaev, S.R. (2010). A method and server for predicting damaging missense mutations. Nature Methods *7*, 248-249.
9. Hallégot, P., Peteranderl, R., and Lechene, C. (2004). In-Situ Imaging Mass Spectrometry Analysis of Melanin Granules in the Human Hair Shaft. Journal of Investigative Dermatology *122*, 381-386.
10. Günther, T., and Coop, G. (2013). Robust identification of local adaptation from allele frequencies. Genetics *195*, 205-220.